Future Foods 6 (2022) 100185

Contents lists available at ScienceDirect

Future Foods

journal homepage: www.elsevier.com/locate/fufo

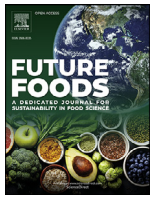

Physicochemical and rheological properties of commercial almond-based yoghurt alternatives to dairy and soy yoghurts

Bhanu Devnani[a,b], Lydia Ong[a,b], Sandra E Kentish[a], Peter J Scales[a], Sally L Gras[a,b,*]

[a] Department of Chemical Engineering, The University of Melbourne, Parkville, VIC 3010, Australia
[b] The Bio21 Molecular Science and Biotechnology Institute, The University of Melbourne, Parkville, VIC 3010, Australia

1. Introduction

Almonds and other plant-based ingredients are increasingly being used to make yoghurt to supply a growing global vegan/non-dairy yoghurt market. These products differ significantly from traditional fermented dairy products that are derivatives of animal milk, although they are formulated to resemble dairy products, including a gel like structure and similar flow behaviour. Almond-based yoghurt alternatives, referred to as almond yoghurt herein, rank second in consumption to soy yoghurt globally (Grand View Research, 2020). These products are typically obtained by blending raw or roasted almonds with water to develop a nut milk base, which is then supplemented with sugar to assist fermentation (Bernat et al., 2015a, 2015b; Shi et al., 2020). Almond yoghurts utilise the protein (14–26%), fat (44–61%) and micronutrients (Yada et al., 2011) of almonds, which can confer favourable nutritional, organoleptic and functional properties (Burns et al., 2016). Although it is not clear how these components contribute to the structure and function of almond yoghurt products and how these products differ from fermented dairy and soy products.

Protein is a major determinant of dairy yoghurt microstructure and the type of proteins present in almond milk differ considerably to the proteins found in animal or soy milk. Amandin is the dominant almond protein, representing ~65–70% of the total soluble protein (Wolf and Sathe, 1998). This ~14 nm globular protein (Sathe et al., 2002) has a molecular mass of ~ 370–427 kDa and consists of 6 prunin subunits (Albillos et al., 2009; Sathe et al., 2002). The casein micelle present in animal milk, is much larger than amandin, being ~200 nm in size and binds calcium phosphate (Bhat et al., 2016). Casein micelles have a molecular mass of ~ 10^5 kDa, consisting of ~ 10^4 monomers of α, β, κ caseins (Dewan et al., 1974), which assemble to form a protein network in fermented dairy products (Lee and Lucey, 2010). Two major proteins are present in soymilk (>70%) (Nik et al., 2009); glycinin, which is ~ 320 kDa in size, has some structural similarities to amandin (Badley et al., 1975) but β-conglycinin, is a trimeric glycoprotein, with a molecular mass of ~ 180 kDa (Nik et al., 2009). The differences in protein structure and aggregation properties between amandin, dairy and soy milk preparations are expected to give varied microstructure.

Protein concentration also plays a critical role in the development of gelled products, such as yoghurt. Previously, almond protein concentration has ranged from 1.4 to 2.8% w/v in studies of almond yoghurts (Bernat et al., 2015a, 2015b), which is lower than the minimum protein concentration of ~3.6% w/v required for heat induced gelation of almond milk, as well as the protein content (> 3% w/v) typical of bovine yoghurt (Devnani et al., 2020; Tamime et al., 2014). This low protein concentration likely explains why weak gels have been obtained following fermentation, leading to a texture that does not resemble dairy yoghurt. A recent study showed the promise of increasing almond protein and fat content (up to 6% w/v and 5% w/v respectively), leading to improved yoghurt texture, increased apparent viscosity and decreased whey separation (Zhao et al., 2021). The textural and flow properties were still reduced, however, compared to dairy yoghurt (Nguyen et al., 2017; Zhao et al., 2021).

Several strategies have been employed to achieve a desirable texture in almond yoghurts. Attempts have been made to strengthen the network structure of almond yoghurt gels by fortification with whey protein and blending with xanthan gum and pectin (Shi et al., 2020) or by combining with bovine skim milk (Yilmaz- Ersan and Topcuoglu, 2021). The inclusion of dairy ingredients, however, prevents consumption by a broader market, including vegans. In commercial products, a low concentration of almond protein (typically 1.4–3.3% w/v), is often combined with stabilisers and thickeners (Tables 1 and S1, Supplementary Information), to achieve the desirable consistency and/or reduce product cost. Particle size and rheological properties are also of further interest for almond yoghurts, including commercial formulations, as these are key determinants of consumer perception.

A recent study examined advances in a variety of commercial plant-based yoghurt alternatives (soy, coconut, cashew, almond and hemp), including their composition and flow properties (Grasso et al., 2020). The textural properties of almond yoghurt made at laboratory scale have also recently been characterized (Zhao et al., 2021). The link between structural and functional properties of commercial almond yoghurts, however, has not been examined. It is also not clear how commercial almond yoghurts differ in their microstructure, rheological and lubrication properties and how these properties compare to traditional products, such as dairy and soy yoghurt.

* Corresponding author at: Department of Chemical Engineering, The University of Melbourne, Parkville, VIC 3010, Australia.
E-mail address: sgras@unimelb.edu.au (S.L. Gras).

https://doi.org/10.1016/j.fufo.2022.100185
Received 29 July 2022; Received in revised form 8 September 2022; Accepted 10 September 2022

The objective of this study was to assess and compare the structural and flow properties of three commercial almond yoghurts commonly available in the Australian market, including the microstructure, particle size, stability, flow and lubrication properties. A second aim was to compare these properties to conventional dairy yoghurt and soy yoghurt, an important plant-based benchmark product, which has the largest share of the vegan yoghurt market (> 45%; Grand View Research, 2020). We hypothesized that the differences in the types of protein and commercial formulations would lead to products with differing structural and functional properties. Understanding the differences between these products will aid the development of almond yoghurts with either improved or similar textural profiles to dairy yoghurt, resulting in enhanced consumer acceptability.

2. Materials and methods

2.1. Materials and reagents

The yoghurts were purchased from local supermarkets across Melbourne, Victoria, Australia, and were stored at 4 °C. The three almond yoghurts analysed in this study were Wise Bunny almond yoghurt (Natural, 600 g), So Delicious almond yoghurt (Natural with a hint of caramel, 500 g) and Nakula plant -based probiotic yoghurt (Vanilla, 500 g), hereafter referred to as AY1, AY2 and AY3 respectively (Table 1). These were compared to Kingland Greek style soy yoghurt (Natural, 500 g), and Coles Greek style dairy yoghurt (Natural, 1000 g). The sample set represents the only almond-based yoghurts available in the Australian market at the time of research. The Greek style variety of dairy yoghurt was chosen as a comparison, as it has a similar fat content to two of the almond yoghurts (AY2 and AY3). All yoghurts were fermented, as required by Australian and NZ guidelines for yoghurt labelling and were unflavoured, with the exception of AY3, all samples were also tested within 5 days of opening, as no significant changes in properties was detected within this timeframe. Purified water (resistance >18.2 MΩ.cm at 25 °C) was used for all experiments. All chemicals used were of analytical grade.

2.2. pH and titratable acidity

The pH of the samples was measured at ~20 °C using a SevenCompact pH metre (Mettler Toledo Ltd., Victoria, Australia). The titratable acidity (TA) was obtained through colorimetric titration method 942.15 (AOAC, 2016) using a 2% (w/v) phenolphthalein solution in ethanol as an indicator. A 10 g sample was mixed with 10 mL of purified water followed by addition of a few drops of indicator and titrated using 0.1 N NaOH solution. The TA, expressed as percentage lactic acid, was calculated as follows:

$$\text{TA}\ (\%) = \frac{\text{Volume of NaOH (mL)} \times \text{Normality of NaOH} \times \text{MW of lactic acid} \times 100}{\text{Sample mass (g)} \times 1000} \quad (1)$$

where molecular weight (MW) of lactic acid is equivalent to 90 g/mol.

2.3. Microstructure

Confocal laser scanning microscopy (CLSM) was used to visualise the microstructure of the yoghurt samples. A small amount (~0.1 g) of each yoghurt was transferred to a glass slide using a spatula. Stock solutions of three different stains namely FITC (fluorescein isothiocyanate; 1% w/v in dimethylformamide (Peighambardoust et al., 2006)), Fast green FCF (0.1% w/v in water) and Nile red (0.1% w/v in dimethyl sulfoxide) (Ong et al., 2011) were prepared and applied in a three-step staining procedure to stain the starch, protein and fat. The sample was first stained with FITC stock solution and incubated in the dark for a minimum of 45 min at room temperature. Next, the Nile red and FCF stock solutions, diluted 5 times in purified water, were added to the sample followed by a 15 min incubation. After blotting excess stain with tissues, the sample was covered with a 0.17 mm thick glass coverslip and visualised with a 63x oil-immersion objective on an inverted CLSM (Leica SP8, Leica Microsystems, Heidelberg, Germany). The excitation/emission wavelengths for FITC, Nile Red and Fast Green FCF were 488/490–530 nm (set to appear cyan), 488/ 530–590 nm (set to appear red) and 633/660–750 nm (set to appear green) respectively. With these configurations, the starch appears cyan, the fat appears red and the protein, which is both stained by FITC and Fast green FCF, appears greenish blue in CLSM images. Triple channel images (512×512 pixels) were obtained in triplicate for each batch of yoghurt.

2.4. Size distribution

The volume-based particle size distribution was obtained at room temperature using a Mastersizer 3000 (Malvern Instruments Ltd., UK) in Can Hydro EV mode. The yoghurt samples were added to deionised water, which was mixed at 1000 rpm until an obscuration rate of 10% was achieved. An absorbance index of 0.001 was used for all samples. The refractive index for all yoghurts as measured using an Abbe DR-A1 digital refractometer at 20 °C (ATAGO CO. LTD., Tokyo, Japan) was 1.35, except soy yoghurt, which had a refractive index of 1.34.

2.5. Stability and syneresis

The susceptibility of yoghurt samples to syneresis was measured using a LUMiFuge (LUM. GmbH, Berlin, Germany), run at 2300 g for 2 h 15 min. The samples were stored at 4 °C prior to measurement. A gradual increase in the instrument temperature from 4 °C to 14 °C occurred during measurement. The normalised transmission was measured as the percentage of light transmitted through the length of the sample tube, with the dynamic transmission profiles being collected every 30 s, for each yoghurt sample. The rate of change of integral transmission or the percentage of total light transmitted across the length of the tube with time, was used to characterise the rate and extent of separation and taken as a measure of yoghurt stability.

For quantification of syneresis, 10 g of each sample (stored at 4 °C) was centrifuged at 4 °C at 2300 g for 20 min. The supernatant was

Table 1
Ingredients of yoghurt samples as noted on the packaging.

Samples	Sample code	Ingredients
Wise Bunny Almond Yoghurt (Natural; 600 g)	AY1	Water, almonds (10%), sugar, stabilisers (maize starch, pectin), live cultures
So Delicious Almond Yoghurt (Natural with a hint of caramel; 500 g)	AY2	Almond milk (water, almonds (14%)), water, sugar, starch (tapioca, rice), apple and hibiscus concentrate, salt (0.1%), lemon pulp, natural flavours, vegan cultures
Nakula Plant-based Probiotic Yoghurt (Vanilla; 500 g)	AY3	Water, coconut, cashews, almonds, native starch, cane sugar, guar gum, live vegan cultures Vanilla blend 8%: water, cane sugar, native starch, natural flavour, vanilla bean seeds (0.2%), acidity regulator (malic acid)
Kingland Greek Style Soy Yoghurt (Natural; 500 g)	SY	Water, soybeans, canola oil, sugar, thickeners (1442-hydroxypropyl distarch phosphate, 412- guar gum, 509- $CaCl_2$), preservative (202), vanillin flavour, live yoghurt cultures
Coles Greek Style Dairy Yoghurt (Natural; 1000 g)	DY	Skim Milk, cream (milk), milk solids, cultures

weighed and the% syneresis was calculated using the following equation:

$$\text{Syneresis (\%)} = \frac{\text{Weight of supernatant x 100}}{\text{Weight of sample}} \quad (2)$$

2.6. Rheological measurements

Rheological measurements were conducted at temperatures of 4 °C and 37 °C using a Discovery HR-2 Hybrid rheometer (TA Instruments, New Castle, USA), where the temperature was controlled by a Peltier temperature control unit and a water thermo-circulator system. A 40 mm parallel plate geometry with a gap of 1000 μm was used for all measurements.

Flow curves were obtained at 4 °C in a shear rate range of 0.1 s^{-1} to 100 s^{-1} to measure the thixotropic behaviour. All samples were stored at 4 °C prior to the measurements. Each sample was first pre-sheared at 100 s^{-1} for 30 s and allowed to re-equilibrate for a duration of 300 s. The shear rate was then increased logarithmically from 0.1 s^{-1} to 100 s^{-1}, held at 100 s^{-1} for a duration of 5 s and logarithmically decreased from 100 s^{-1} to 0.1 s^{-1}. Thixotropy (Pa/s) was defined as the hysteresis between the upward (increasing shear rate) and downward (decreasing shear rate) curves. A power law was fitted to the increasing shear rate data to obtain the values of consistency index (K) and flow index (n), which were then used to calculate the apparent viscosity at 50 s^{-1} (η_{50}).

Flow curves and frequency sweeps were collected at 37 °C using the method of Nguyen et al. (2017) to allow further comparisons with tribological behaviour (Section 2.7). Samples were incubated at room temperature (~24 °C) for 1 hour and gently stirred using a stainless-steel spatula (10 times in one direction) prior to measurement. To obtain the flow curve, each sample was first conditioned at 37 °C for 60 s followed by a logarithmic shear rate sweep from 0.1 s^{-1} to 1000 s^{-1}. Storage and loss moduli of the yoghurt samples were obtained by conducting frequency sweeps in the linear viscoelastic region. The sample was first preconditioned at 37 °C for 60 s, following which the frequency was increased from 0.1 rad/s to 100 rad/s at a strain of 0.1%. The solvent trap of the standard Peltier plate (TA instruments), filled with distilled water, along with the solvent trap cover, were used to prevent/minimise evaporation during measurements.

2.7. Tribological measurements

To simulate the oral processing conditions, tribological measurements were conducted at 37 °C on a Discovery HR-2 Hybrid rheometer using a ring on plate tribo-rheometry geometry, following the method of Nguyen et al. (2017) with minor modifications. Briefly, a sample layer of approximately 1 mm thickness was spread onto the lower plate covered with a 3 M Transpore Surgical Tape (3 M health Care, USA) and the geometry lowered until an axial force of 2 N was reached. Samples were then conditioned at 24 °C, where pre-shearing at 0.01s^{-1} was carried out followed by equilibration, each for a duration of 60 s. This was followed by a flow sweep at 37 °C where the frequency was increased logarithmically from 0.01 rad/s to 100 rad/s. All samples were stored at room temperature (~24 °C) 1 h prior to tribological measurements.

The data points where the normal force deviated for more than 5% of the set value (2 N) were eliminated while plotting the coefficient of friction against the entrainment speed (μm/s).

2.8. Statistical analysis

All properties were measured three times in replicate measurements and averaged for each batch of yoghurt. Two independent batches of yoghurt were analysed for each type of yoghurt and results expressed as mean of the two average values ($n = 2 \pm$ the standard deviation). The means for the different types of yoghurt samples were then compared by one-way analysis of variance (ANOVA) using SPSS software with a significance of 95%. Tukey's test was used to detect pairwise significant differences.

3. Results and discussion

3.1. Ingredient and nutritional profile

The set of commercial yoghurts selected for analysis included non-dairy yoghurts AY1 and AY2 based on almonds, as well as AY3, an almond product that also contained coconut and cashews (Table 1). A range of stabilizers, including gums (guar gum), pectin and native or modified starch, sourced from different crops (maize, rice, tapioca) were present in these plant-based yoghurts. These stabilisers were absent in the conventional dairy yoghurt, which also contained the least number of ingredients.

The fat: protein ratio of AY1 and AY2 products is ~ 2.3:1 (Table 2) and reflects the natural composition of fat (45–55% w/w) and proteins (18–24% w/w) in almonds (Yada et al., 2013, 2011). AY2 contained the highest almond content (14% in AY2 versus 10% w/w in AY1; Table 1) resulting in a greater concentration of both fat and protein (Table 2). AY3, had a higher concentration of both total and saturated fat, due to the presence of coconut and cashews, with a total fat content similar to dairy yoghurt ~9% w/w. In contrast, most of the fat in AY1 and AY2 was unsaturated, as mono and polyunsaturated fatty acids constitute ~ 90% of the total lipids in almonds (Yada et al., 2011).

Though almonds are protein rich, the concentration of almonds (10–14% w/w) used in these products resulted in a protein content of 1.8–2.7% w/w, which is almost half the protein concentration in soy and dairy yoghurt (~5% w/w) (Table 2). This low protein concentration is important, as in dairy products the texture is directly related to the formation of a cross-linked protein gel (Lee and Lucey, 2010). The sugar content in all almond yoghurts (4–7% w/w) was similar to in dairy yoghurt (5.5% w/w) but the polysaccharides added increased the total carbohydrate content of these yoghurt products considerably (9–11% versus 7% w/w in dairy). Despite different formulations, AY2 and AY3 had a similar total solids content to dairy yoghurt (~21% w/w), while AY1 and the soy yoghurt had lower total solids (14.9% and 11.5% w/w, respectively). Although almonds are known to contain 200–400 mg of calcium/100 gm (Yada et al., 2013), the calcium content was not declared the three almond products examined here.

The similarity of the ingredient and nutritional profile used in the current study to other almond yoghurts available internationally (Table S1, Supplementary Information), indicates that these samples are representative of the majority of the almond yoghurts currently available in the global market.

3.2. pH and titratable acidity (TA)

The pH was similar for all yoghurts (Table 2), with the TA being significantly lower for all plant-based yoghurts than for the dairy yoghurt (Table 2), consistent with prior studies (Grasso et al., 2020). This difference can be attributed to the higher buffering capacity of cow's milk relative to almond and soy beverages, arising from the higher protein concentration (4.9% in bovine milk versus < 1% in almond milk) and naturally occurring salts and organic acids present in bovine milk (Lee et al., 2018; Salaün et al., 2005). The differences in TA between almond yoghurts AY1-AY3 reflect the different product composition (Table 2), as protein, organic acids and minerals are known to give better buffering capacities (Mennah-Govela and Bornhorst, 2021) and sugar type, bacteria and fermentation conditions also impact on buffering capacity and acidic metabolites (Abedi and Hashemi, 2020; Szparaga et al., 2019; Trontel et al., 2010). Acidic ingredients added after fermentation (e.g. lemon pulp added to AY2) are also expected to increase TA.

Though some studies have shown the TA to be positively correlated to a perceived sourness at a similar pH (Da Conceicao Neta et al., 2007;

Table 2
Physicochemical properties of yoghurt samples: Composition (per 100 g) as noted on the packaging; pH and titratable acidity (TA) measured at 20 °C.

Sample code	Total fat/of which saturated (g)	Protein (g)	Carbohydrate/ of which sugar (g)	Ca (mg)	Total solid (%)	pH	TA (%)
AY1	3.7/0.3	1.8	9.4/5	NA	14.9	4.01 ± 0.01 [a]	0.52 ± 0.02 [b]
AY2	7.1/0.6	2.7	10.9/6.8	NA	20.7	3.99 ± 0.09 [a]	0.70 ± 0.00 [a]
AY3	9.2/3.8	2.5	9.8/4.3	NA	21.5	4.00 ± 0.01 [a]	0.37 ± 0.01 [c]
SY	4.0/<1	4.8	2.7/1.8	NA	11.5	4.23 ± 0.07 [b]	0.79 ± 0.00 [d]
DY	9.5/6.8	4.9	6.7/5.5	169	21.1	3.89 ± 0.01 [a]	1.78 ± 0.05 [e]

NA: Not available.
Different superscripts indicate significant differences ($p < 0.05$) between the mean values within each column.

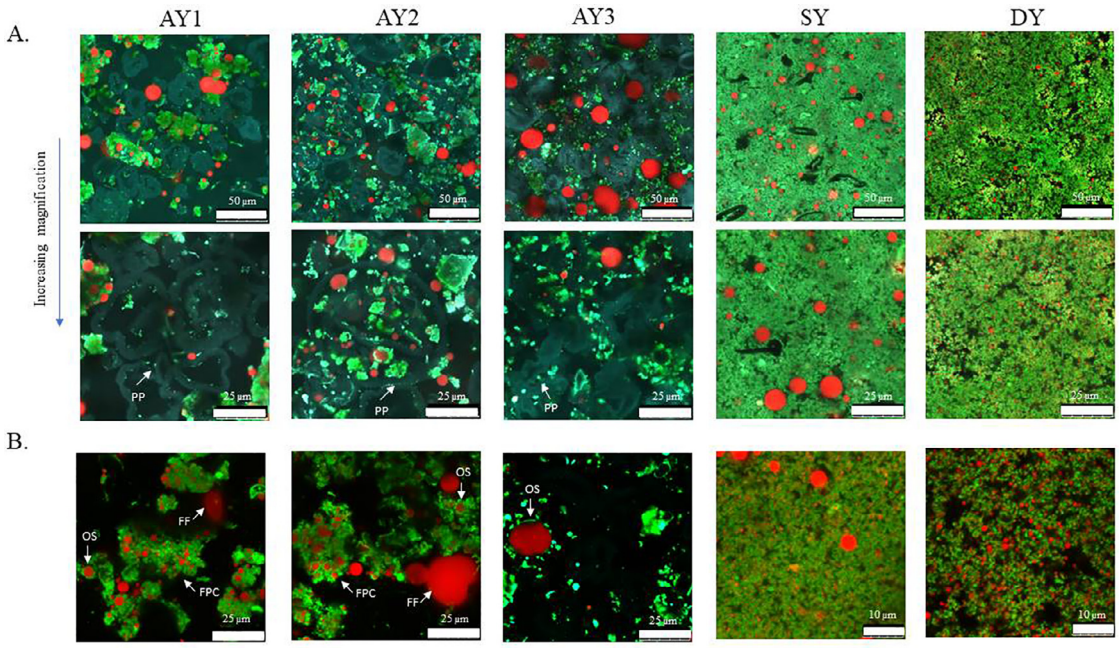

Fig. 1. Microstructure of yoghurt samples determined by confocal microscopy. Tricolour staining **(A)** to visualise the overall sample microstructure, where fat, protein and starch appear red, green and cyan respectively. Bicolour staining **(B)** to visualise interactions between fat and protein, where fat and protein appear red and green. PP = protein particles associated with the starch granules, FPC = fat-protein clusters, FF = free fat and OS = oleosome. Sample codes are as described in Table 1.

Tyl and Sadler, 2017), further studies are required to establish this association in plant-based systems.

3.3. Microstructure

The microstructure of the almond yoghurts was heterogenous, containing flocculated particles of protein, fat globules, aggregates of fat and protein and starch granules of varying size and shape (Fig. 1A, AY 1,2,3). The unstained regions are expected to contain ingredients not stained by FITC, FCF and Nile red, such as pectin and gums, that are dispersed in the aqueous phase.

Starch granules appear cyan in colour and swollen as a result of water absorption in all three almond yoghurts, as has been observed previously in other starch containing food systems (Matignon et al., 2014). Some fine green stained protein particles associated with the walls of the swollen starch granules, were evident in the higher magnification images (Fig. 1A, PP). Several dense clumps of fat and protein were also present in these samples (Fig. 1B, FPC). There was little evidence of interaction between these clumps, indicating that they may have formed through hydrophobic interaction upon protein denaturation and/or aggregation during processing. Examples of free fat were also observed in the matrix (Fig. 1B, FF), suggesting that either the fat was not fully homogenized during production or that the fat partially coalesced during or following production. The protein lining observed around some of the fat globules also indicate that these may be intact oleosomes (or oil bodies lined with a protein and phospholipid membrane) (Fig. 1B; AY 1,2,3; OS), that are naturally known to occur in nuts and their extracts (Bastiaan-Net, 2020; Dave et al., 2019; Gallier et al., 2012).

In contrast, both the soy and dairy yoghurts demonstrated a continuous and porous protein network (Fig. 1A and B; SY, DY), with a higher porosity being observed for dairy yoghurt compared to soy yoghurt. Irregularly shaped unstained regions were evident in the soy yoghurt (Fig. 1 A; SY), which may contain unstained stabilisers (guar gum and modified starch). The modified starch, which was present in soy yoghurt but not the dairy yoghurt, could not be visualized with FITC, as the chemical changes occurring during starch modification are expected to limit dye binding (EFSA Panel on Food Additives and Nutrient Sources added to Food et al., 2017; Chin et al., 2014; Eliášová et al., 2012). No swollen starch granules were observed in either of the dairy or soy yoghurts.

Another interesting feature, demonstrating the degree of homogenisation, was the length scale at which fat globules could be clearly observed in these samples (Fig. 1B, SY and DY were digitally zoomed 4x compared to 2x zoom in AY 1,2,3). The fine fat particles (< 1 µm in size) in soy yoghurt and dairy yoghurt, that were integrated within the protein network, were evident only at higher magnification (10 µm) (Fig. 1B, SY and DY). This integration of fat droplets into the protein network is consistent with prior reports of soy and dairy yoghurt, that suggest fat-protein clusters formed in these systems following homogenisation interact during the fermentation process to form a continuous net-

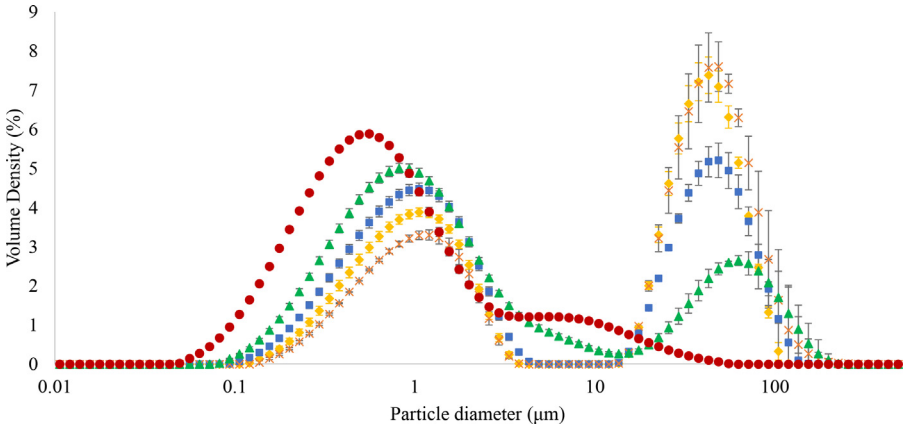

Fig. 2. Particle diameter distribution of yoghurt samples AY1 (♦), AY2 (■), AY3 (×), SY (▲) and DY (●) measured at 20 °C. Sample codes are as described in Table 1. Error bars represent the standard deviation of the mean (n = 2).

work (Nguyen et al., 2014; Yazici et al., 1997). Larger fat globules of up to 2 μm in size, embedded within the serum containing pores (Fig. 1B, SY and DY), were also seen in both yoghurts. Additionally, even bigger fat particles of up to 10 μm diameter were observed within soy yoghurt (Fig. 1A and B, SY), perhaps due to the addition of canola oil in the formulation.

Overall, while a fine interconnected protein network was responsible for structuring the gel in soy and dairy yoghurts, no specific structural organization existed in any of the almond yoghurts, which contained heterogeneous structures embedded in an aqueous phase containing ingredients such as pectin and gums. The mechanism of gelation for the almond yoghurts is not clear from the images. The gel characteristics, synaeresis and rheology were therefore examined to better understand the functional properties of these gels.

3.4. Size distribution

The volume-based size distribution of single particles and/or macromolecular aggregates in the yoghurt gels was measured following stirring in distilled water (Fig. 2). This approach measures species larger than 0.1 μm but is less able to detect finer protein particles. These larger particles >0.1 μm are known to affect the stability and texture of yoghurt, influencing sensory properties and consumer perception (Cayot et al., 2008; Lee and Lucey, 2010).

A bimodal distribution of particle sizes was measured for all samples. The position of the two peaks was similar for all three almond yoghurts (Fig. 2). The first peak at ~1 μm likely corresponds to weakly associated protein particles/ aggregates that dissociate on dilution and stirring. The second peak at ~42 μm likely represents the swollen starch granules and fat-protein clusters observed in the confocal images (Fig. 1) and the unstained polysaccharides (pectin, gums and fibre) present in the matrix. Swollen starch granules of maize, tapioca and rice are known to range between 15 and 35 μm, 20- 48 μm, 4–13 μm in diameter respectively depending on the starch composition and degree of gelatinisation (Li et al., 2008; Li and Yeh, 2001; Rao and Tattiyakul, 1999; Zhang et al., 2017; Ziegler et al., 1993).

The dairy yoghurt contained ~0.5 μm particles, smaller than the ~1 μm particles present in soy yoghurt (Fig. 2). An additional shoulder was obtained in the particle size distribution for both these yoghurts (4–50 μm for DY and 3–12 μm for SY), potentially arising due to the higher degree of protein gelation, consistent with the more continuous protein network observed by CLSM (Fig. 1). The second peak in SY at ~60 μm may be the result of either bigger fat particles and/or the added hydrocolloids.

In general, the average particle size of almond based systems was larger than soy and dairy based systems. All particles measured were below 150 μm in size, so are smaller than the size known to negatively affect the sensorial properties of yoghurt (Cayot et al., 2008). The particle size differences observed here, however, are expected to influence the rheological and lubricating properties of yoghurt samples, both of which influence the sensory perception.

3.5. Stability and syneresis

No visible separation was encountered in any of the yoghurt samples, so the stability of yoghurt samples against serum separation was measured through an accelerated sedimentation technique (Fig. 3). The change of integral transmission through the sample under a centrifugal force with time indicates the rate of sedimentation, with a higher gradient corresponding to lower stability.

No syneresis was observed in either the soy or dairy yoghurt, consistent with the gel structure being dominated by an interconnected protein network (Fig. 3). The high fat and protein content in the dairy yoghurt and the presence of hydrocolloids in the soy yoghurt, may have further enhanced the gel strength of these samples, as reported in prior studies (Grasso et al., 2020; Lee and Lucey, 2010; Nguyen et al., 2017).

Out of all the yoghurts tested, only AY1 and AY2 underwent serum separation (Fig. 3). This behaviour is consistent with these gels being dominated by flocculated particulate aggregates (Fig. 1A). AY1 had lower stability (Fig. 3) and exhibited higher synaeresis (22 ± 2%; w/w) than AY2 (3 ± 0%; w/w), probably due to its ~30% lower total solids content (Table 2) and ~60% greater number of large particles (Fig. 2). The syneresis values were much lower than those previously reported for fermented almond milk (50–60%; v/v) (Bernat et al., 2015a), probably due to the action of the stabilizers and gum components added to these formulations, which are expected to effectively reduce syneresis (Tasneem et al., 2014).

Though AY3 had a similar amount of total solids as AY2 (Table 2), the compositional differences between these two formulations, including the nut milk base and the stabiliser blend, successfully prevented syneresis in AY3. The two potential reasons contributing to restricted water mobility in AY3 during centrifugation include the presence of a) saturated fat from coconuts (melting range 17- 32 °C; Tipvarakarnkoon et al. (2008)) and cashews (melting point 16–19 °C; Yahaya et al. (2012)), which were solid at the measurement temperatures of 4–14 °C and b) guar gum, which may have formed a polymeric gel, thus strengthening the gel structure.

In summary, the lower stability of AY1 and AY2 is consistent with these gels being particulate flocculated structures (Fig. 1). The behaviour of AY3 is consistent with a network dominated by a molecular gel (gum-based), although an aggregated particulate network is observed in CLSM images (Fig. 1). In contrast, the soy and dairy yoghurts contain a crosslinked protein or molecular network, which is stable against sedimentation.

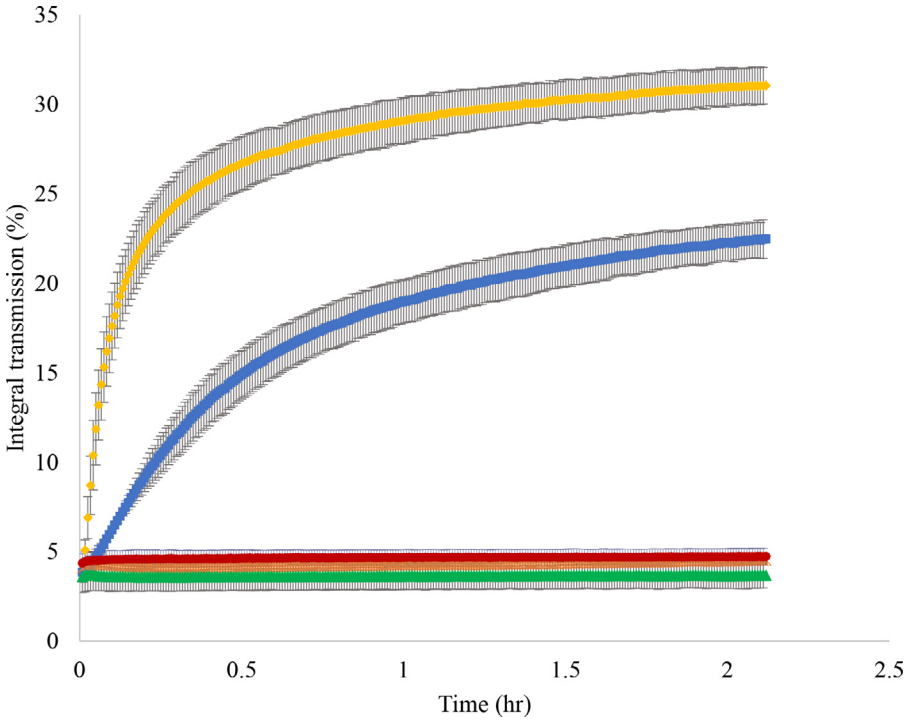

Fig. 3. Physical stability of yoghurt samples AY1 (♦), AY2 (■), AY3 (×), SY (▲) and DY (●) as measured through accelerated sedimentation at 2300 g for 2 hrs 15 min. Sample codes are as described in Table 1. Error bars represent the standard deviation of the mean ($n = 2$).

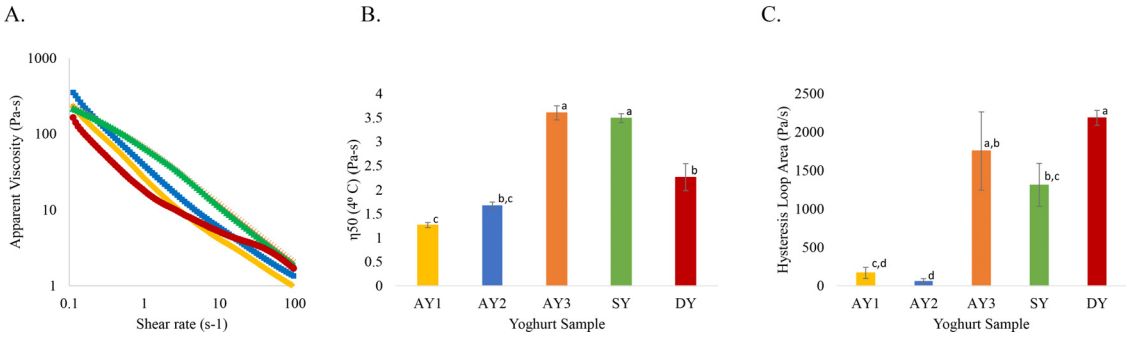

Fig. 4. Rheological properties of yoghurt samples at 4 °C. The flow curve of yoghurt samples AY1 (♦), AY2 (■), AY3 (×), SY (▲) and DY (●) **(A)** and the apparent viscosity at a shear rate of 50 s^{-1} (η_{50}) (Pa-s) **(B)** when the shear rate was increased from 0.1 s^{-1} to 100 s^{-1}. Hysteresis loop area (Pa/s) **(C)** obtained by increasing the shear rate from 0.1 s^{-1} to 100 s^{-1}, holding at 100 s^{-1} and then decreasing the shear rate from 100 s^{-1} to 0.1 s^{-1}. Different superscripts in each graph indicate significant differences ($p < 0.05$) between the samples. Sample codes are as described in Table 1.

3.6. Apparent viscosity and thixotropy (4 °C)

The viscous and flow hysteresis properties of yoghurt at 4 °C provide important insights into the product stability to shear stresses generated during transportation and handling, as well as during consumption. All samples were shear thinning (Fig. 4A) and a power law function could be effectively fitted to the data (R^2 of 0.90- 0.99; Table S2, Supplementary Information).

The apparent viscosity at a shear rate of 50 s^{-1} (η_{50}) value was chosen to compare different samples, as this value is suggested to correlate with consumer perception of thickness in food products (Wood, 1968) (Fig. 4B). The η_{50} values obtained for AY1 and AY2 were slightly lower than the η_{50} value obtained for dairy yoghurt (~2.3 ± 0.3 Pa-s), which was consistent with the range of ~2–2.4 Pa-s reported previously in the literature (Jeske et al., 2018). Similar η_{50} values were detected for AY3 and soy yoghurt, these being clearly higher than measured for the dairy yoghurt. This suggests that AY1 and AY2 are expected to be thinner than AY3, soy and dairy yoghurt.

The samples differed in their shear recovery behaviour, with negligible hysteresis between the upward and downward shear rate loops being observed for AY1 and AY2 (Figs. 4C; S1, Supplementary Information), highlighting the resilience of these almond samples to structural deformation. This behaviour is consistent with flocculated, hard particle systems, such as coagulated alumina suspensions, where the interparticle interactions, dominated by Van der Waal forces, aid in the immediate regeneration of the structure upon shear removal (Kumar et al., 2012). Though AY3 shared a similar microstructure to AY1 and AY2, this yoghurt demonstrated a higher hysteresis loop area, statistically comparable to that of soy and dairy yoghurt (Fig. 4C). A potential reason for this difference could be the solidification of the saturated fat present in this formulation, which along with the stabiliser blend, restricted the flow and structural recovery upon deformation. The high hysteresis loop area of soy and dairy yoghurt was concordant with prior observations (Nguyen et al., 2014; Shen et al., 2021). Such behaviour is typical for cross-linked gelled systems, where the structural recovery is

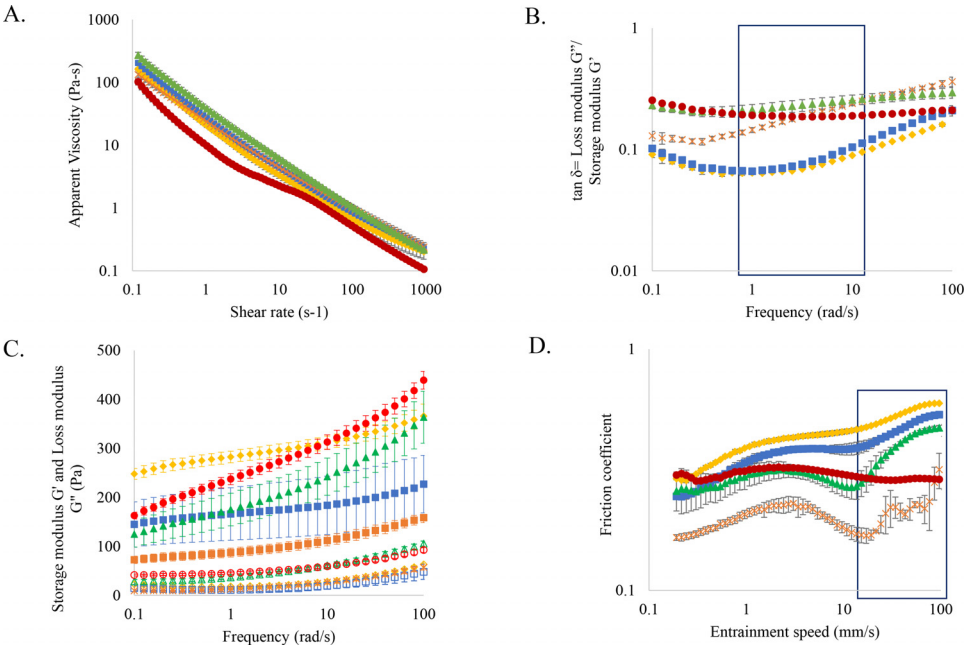

Fig. 5. Rheological and tribological characterisation of yoghurt samples AY1 (♦), AY2 (■), AY3 (×), SY (▲) and DY (●) at 37 °C. **(A)** Apparent viscosity measured over a shear rate of 0.1 s^{-1} to 1000 s^{-1}, **(B)** tan δ measured over a frequency of 0.1 rad/s to 100 rad/s, **(C)** Storage modulus G' (Pa) (filled symbols) and loss modulus G" (Pa) (empty symbols) of yoghurt samples measured as a function of increasing frequency from 0.1 rad/s to 100 rad/s at 37 °C, and **(D)** the coefficient of friction measured as a function of entrainment speed of 0.1 mm/s to 1000 mm/s. The boxes in (B) and (D) highlight regions where a similar trend is observed for the tan δ and friction profiles of all samples across the frequency range of 1–10 rad/s or entrainment range of 10–100 mm/s respectively i.e. an upwards trend for all samples other than dairy yoghurt. Sample codes are as described in Table 1. Error bars represent the standard deviation of the mean ($n = 2$).

time-dependant and reflects the reformation of bonds in an entangled molecular network within the system.

3.7. Rheological and tribological properties (37 °C)

At 37 °C, the η_{50} values measured for the almond and soy yoghurts were statistically comparable (Fig. S2, Supplementary Information), suggesting the products were likely designed to have similar viscosities and mouthfeel at a temperature relevant to consumption. The viscosities were all within the range previously reported for dairy yoghurt (0.2–1.2 Pa-s) (Nguyen et al., 2017). This similarity contrasts with the significantly different viscosity (η_{50} values) measured for chilled products at 4 °C (Fig. 4B). In general, higher viscosities in both dairy and plant-based yoghurts, have been linked to enhanced perception of thickness, smoothness, mouth coating and flavour, all of which have been shown to positively influence product perception (Dickinson, 2018; Greis et al., 2020).

Despite similarities in viscosity, the viscoelastic properties of the five products differed (Fig. 5A–C). The plant-based yoghurts became more liquid-like with increasing shear, as indicated by the rising tan δ values as a function of frequency (Fig. 5B). The extent of shear thinning, as indicated by the slope of the curve, was higher for almond yoghurts, as compared to the soy yoghurt. This behaviour is potentially due to the absence of an organized protein-based network structure, which is present in soy and dairy yoghurts (Fig. 1). In short, the data is consistent with the plant-based gel behaviour being dominated by particulate interactions. The slight increase observed for soy yoghurt could be because of the added gelling agents. Similar behaviour has been observed in dairy yoghurts, where the addition of modified starch at certain concentrations was found to lower the gel strength (Nguyen et al., 2017). Differences in composition, including the type of fat (unsaturated in soy vs saturated in dairy), amount of fat (lower in soy) and size of fat globules (higher in soy) may also have contributed to this behaviour. Further, the gel strength/ elastic moduli G' (Pa) of almond yoghurts AY1–3 (Fig. 5C) seemed to decrease significantly ($p < 0.05$) (AY1> AY2> AY3) with increasing fat content (AY1< AY2< AY3). The fat interspersed within the particulate network could make deformation easier in the almond yoghurt with higher fat.

In contrast to all plant-based alternatives, there was little change in the tan δ values of dairy yoghurt as a function of frequency, indicating greater structural stability. This could be attributed to the higher fat content and the smaller fat globules present in the dairy yoghurt, both of which are known to strengthen the three-dimensional protein network system (Lee and Lucey, 2010; Truong et al., 2016). Specifically, the presence of smaller fat globules in a dairy yoghurt leads to a higher surface area, increasing protein-fat interactions. The adsorption of proteins on the fat particles, makes them effectively act as protein particles, increasing the cross-linking density of these acid gels.

The tribological behaviour, which was examined as an indicator of yoghurt smoothness, also differed across samples (Fig. 5D). Variations were observed between the almond systems, perhaps due to different formulations. A much higher friction was observed in almond systems AY1 and AY2, at all entrainment speeds, compared to soy and dairy, potentially due to the presence of larger particles, as observed in Figs. 1 and 2. The almond yoghurt AY3, in contrast, offered lower friction, probably because of its higher fat content. The type and concentration of added gelling agents might also have influenced this behaviour, as they have been known to influence the lubricating properties of dairy and soy-based acid gels (Nguyen et al., 2017; Pang et al., 2020). The frictional profile observed for dairy yoghurt here, was concordant with prior studies (Nguyen et al., 2017), with the profile of soy yoghurt being closest to that of dairy, perhaps due to structural similarities (Fig. 1, SY and DY).

In the initial stages of oral processing, the lubrication properties are known to be governed by the bulk rheological properties (Prakash et al., 2013). In this study, the change in friction coefficients within the entrainment speed range of 10–100 mm/s (Fig. 5D, box), seemed to correlate with the viscoelastic properties at corresponding frequencies (Fig. 5B, box), i.e., an upwards trend for all samples other than dairy yoghurt, which remained near constant. Hence, even though the apparent viscosity profiles of all samples were similar (Fig. 5A), the differences existing in the viscoelastic and lubrication properties (Fig. 5B, C and D) are expected to influence the sensory properties of these yoghurts. Further studies are required, however, to determine the impact of various ingredients present in the formulations on these properties and to establish a correlation between the instrumental measurements made and consumer sensory evaluation.

In addition, flavour plays a critical role in consumer acceptability of a food product and the relationship between flavour and texture is also important (Tournier et al., 2007). The characteristic flavour and texture of traditional dairy yoghurt is a function of the dairy ingredients, including the milk fat, protein and carbohydrates and the presence and metabolism of lactic acid bacteria during fermentation (Chen et al., 2017). While this flavour- texture relationship and its influence on consumer physiology has been well researched for dairy systems (Gierczynski et al., 2011), similar studies are required for fermented almond-based systems, due to the compositional differences of almond and dairy ingredients and the textural differences that can arise from structural differences in the networks formed by these proteins.

Structurally and in flow, the almond yoghurts examined here by CSLM and rheology, appear to behave like flocculated gels lacking a continuous and organized protein-based molecular network, as in the dairy and soy yoghurt (Fig. 1). At a higher temperature of 37 ˚C, similar viscosities were obtained for all yoghurts but the viscoelastic or gel properties of almond yoghurts differed, potentially because of their underlying differences in their gel structures, which also influenced lubrication (Fig. 5). Despite the similar appearance of the structure of all three almond yoghurts, differences in formulation, including the addition of cashew and coconut fat, led to variations in texture and stability between these yoghurts (Figs. 4 and 5). AY1 and AY2 exhibited higher tendency for synaeresis (Fig. 3), had a lower viscosity and higher structural recovery at 4 ˚C (Fig. 4), as compared to soy and dairy yoghurt. AY3, in contrast, had similar stability (Fig. 3), viscosity and flow hysteresis properties to soy and dairy yoghurts at 4 ˚C (Fig. 4), potentially because of a higher fat content. Although AY2 and AY3 had a similar particle size distribution (Fig. 2), it is interesting to note that their ingredient and compositional differences (Table 1) resulted in different functional properties, including physical stability (indicated by sedimentation; Fig. 3) and rheological properties including hysteresis (Fig. 4C) and storage modulus (Fig. 5B), indicating that particle size was less significant than these factors in determining functional properties.

Overall, of the three almond formulations studied, AY3 most closely resembled the properties of dairy and soy yoghurts, which is likely due to the higher fat content of this product. AY3 stability and hysteresis were more like dairy (Figs. 3, 4), although not all gel properties were similar (Figs. 4 and 5). Future almond formulations that are able to form an interconnected protein network structure that is dairy-like at the micro-scale (Fig. 1) are expected to display a wider range of dairy-like gel properties, leading to enhanced consumer acceptability.

Almond proteins behave differently in a typical dairy yoghurt making process (Devnani, 2021), as they differ to casein micelles in composition, structure and their propensity for denaturation. One route to potentially create a more dairy-like crosslinked network structure, may be to modify the physical properties of almond proteins through heat induced denaturation (Devnani et al., 2020), high pressure processing (Sim et al., 2020), chemical acid induced denaturation (Devnani et al., 2021) or enzymatic treatment (Zhao et al., 2022). These treatments may be used alone or in combination to alter almond protein properties and network formation with the goal of achieving a protein-based gel that behaves less like a flocculated gel and more like an organized protein network. Almond protein concentration is a further factor critical to gel structuring. Such processing techniques will potentially alter almond protein concentration, which should be kept high, in order to meet the minimum protein concentration required for heat induced gelation (~3.6% w/v; Devnani et al., 2020) and to improve the physical properties of the protein network.

Future studies may also assess potential changes in almond yoghurt properties as a function of extended storage. Although the yoghurt properties measured here appeared stable over the time frame examined (5 days from opening), yoghurt systems are often dynamic. A further study could therefore assess how the structure and properties of flocculated almond gels change during extended storage to further improve our understanding of these complex gel structures.

4. Conclusion

The structural and functional properties of a range of almond-based yoghurt alternatives were examined and compared to dairy and soy yoghurts. The three almond yoghurts all had a low protein content (~2.5%), contained stabilisers and behaved as gels containing large particles or flocs, unlike the dairy and soy yoghurts (~5% protein), which contained an interconnected protein network. Whilst the almond yoghurts had similar apparent viscosities to dairy products at 37 ˚C, their viscoelasticity and lubrication properties differed. Compositional differences also contributed to differences in functionality between almond yoghurt products. Products featuring only almond had lower stability, apparent viscosity at 4 ˚C and hysteresis, whilst products with additional fat better mimicked some dairy properties. This study indicates the need for further product optimisation if almond yoghurt products are to fully mimic all properties of dairy or soy yoghurts. A consideration of almond protein concentration, particle size, network structure and the interaction of component particles could be used to influence functional properties and assist optimisation. Other strategies, such as calcium fortification, could also assist structuring and network formation, whilst increasing nutritional benefits. A further examination of the links between structural and physicochemical properties with sensory perception and study of changes in product properties during storage would also assist the reverse engineering of dairy-like almond yoghurt products.

Ethical statement - studies in humans and animals

The research presented does not involve any animal or human study.

Declaration of Competing Interest

The authors declare that they have no known competing financial interests or personal relationships that could have appeared to influence the work reported in this paper.

Acknowledgement

Dr Bhanu Devnani thanks The University of Melbourne for a Melbourne Research Scholarship. This research did not receive any specific grants from funding agencies in the public, commercial or not-for-profit sectors. Bhanu Devnani, Lydia Ong and Sally Gras were supported by The ARC Dairy Innovation Hub, a collaboration between The University of Melbourne, The University of Queensland and Dairy Innovation Australia Ltd. The authors thank The Advanced Microscopy Facility (AMF), The Biological Optical Microscopy Platform (BOMP) at The Bio21 Molecular Science and Biotechnology Institute and The Particulate Fluids Processing Centre at The University of Melbourne for access to equipment.

Supplementary materials

Supplementary material associated with this article can be found, in the online version, at doi:10.1016/j.fufo.2022.100185.

References

Abedi, E., Hashemi, S.M.B., 2020. Lactic acid production–producing microorganisms and substrates sources-state of art. Heliyon 6 (10), e04974. doi:10.1016/j.heliyon.2020.e04974.

Albillos, S.M., Menhart, N., Fu, T.J., 2009. Structural stability of amandin, a major allergen from almond (*Prunus dulcis*), and its acidic and basic polypeptides. J. Agric. Food Chem. 57 (11), 4698–4705. doi:10.1021/jf803977z.

AOAC, 2016. Official Methods of Analysis of AOAC International. AOAC International, Rockville, MD ISBN: 978-0-935584-87-5.

Badley, R.A., Atkinson, D., Hauser, H., Oldani, D., Green, J.P., Stubbs, J.M., 1975. The structure, physical and chemical properties of the soy bean protein glycinin. Biochim. et Biophys. Acta (BBA)-Protein Struct. 412 (2), 214–228. doi:10.1016/0005-2795(75)90036-7.

Bastiaan-Net, S., 2020. Cracking the Cashew nut: Strategies to Identify Novel Allergens. Wageningen University doi:10.18174/530154.

Bernat, N., Cháfer, M., Chiralt, A., González-Martínez, C., 2015a. Development of a non–dairy probiotic fermented product based on almond milk and inulin. Food Sci. Technol. Int. 21 (6), 440–453. 10.1177%2F1082013214543705

Bernat, N., Cháfer, M., Chiralt, A., González-Martínez, C., 2015b. Probiotic fermented almond "milk" as an alternative to cow-milk yoghurt. Int. J. Food Stud. 4 (2). doi:10.7455/ijfs/4.2.2015.a8.

Bhat, M.Y., Dar, T.A., Singh, L.R., 2016. Casein proteins: structural and functional aspects. In: Milk Proteins–From Structure to Biological Properties and Health Aspects. InTech, pp. 1–17.

Burns, A.M., Zitt, M.A., Rowe, C.C., Langkamp-Henken, B., Mai, V., Nieves Jr,, C., Ukhanova, M., Christman, M.C., Dahl, W.J., 2016. Diet quality improves for parents and children when almonds are incorporated into their daily diet: a randomized, crossover study. Nutr. Res. 36 (1), 80–89. doi:10.1016/j.nutres.2015.11.004.

Cayot, P., Schenker, F., Houzé, G., Sulmont-Rossé, C., Colas, B., 2008. Creaminess in relation to consistency and particle size in stirred fat-free yogurt. Int. Dairy J. 18 (3), 303–311. doi:10.1016/j.idairyj.2007.06.009.

Chen, C., Zhao, S., Hao, G., Yu, H., Tian, H., Zhao, G., 2017. Role of lactic acid bacteria on the yogurt flavour: a review. Int. J. Food Prop. 20 (S1), S316–S330. doi:10.1080/10942912.2017.1295988.

Chin, S.F., Azman, A., Pang, S.C., Ng, S.M., 2014. Fluorescein-labeled starch maleate nanoparticles as sensitive fluorescent sensing probes for metal ions. J. Nanomater. 2014, 108359. doi:10.1155/2014/108359.

Da Conceicao Neta, E.R., Johanningsmeier, S.D., McFeeters, R.F., 2007. The chemistry and physiology of sour taste – a review. J. Food Sci. 72 (2), R33–R38. doi:10.1111/j.1750-3841.2007.00282.x.

Dave, A.C., Ye, A., Singh, H., 2019. Structural and interfacial characteristics of oil bodies in coconuts (*Cocos nucifera L.*). Food Chem. 276, 129–139. doi:10.1016/j.foodchem.2018.09.125.

Devnani, B., Ong, L., Kentish, S., Gras, S., 2020. Heat induced denaturation, aggregation and gelation of almond proteins in skim and full fat almond milk. Food Chem. 325, 126901. doi:10.1016/j.foodchem.2020.126901.

Devnani, B., 2021. The Behaviour of Almond Proteins in purified, Minimally Processed and Complex Food Systems (Doctoral Dissertation. University of Melbourne.

Devnani, B., Ong, L., Kentish, S., Gras, S.L., 2021. Structure and functionality of almond proteins as a function of pH. Food Struct. 30, 100229. doi:10.1016/j.foostr.2021.100229.

Dewan, R.K., Chudgar, A., Mead, R., Bloomfield, V.A., Morr, C.V., 1974. Molecular weight and size distribution of bovine milk casein micelles. Biochim. et Biophys. Acta (BBA)-Protein Struct. 342 (2), 313–321. doi:10.1016/0005-2795(74)90086-5.

Dickinson, E., 2018. On the road to understanding and control of creaminess perception in food colloids. Food Hydrocoll. 77, 372–385. doi:10.1016/j.foodhyd.2017.10.014.

Mortensen, A., Aguilar, F., Crebelli, R., Di Domenico, A., Dusemund, B., Frutos, M.J., Galtier, P., Gott, D., Gundert-Remy, U.EFSA Panel on Food Additives and Nutrient Sources added to Food (ANS), 2017. Re-evaluation of oxidised starch (E 1404), monostarch phosphate (E 1410), distarch phosphate (E 1412), phosphated distarch phosphate (E 1413), acetylated distarch phosphate (E 1414), acetylated starch (E 1420), acetylated distarch adipate (E 1422), hydroxypropyl starch (E 1440), hydroxypropyl distarch phosphate (E 1442), starch sodium octenyl succinate (E 1450), acetylated oxidised starch (E 1451) and starch aluminium octenyl succinate (E 1452) as food additives. EFSA J. 15 (10), e04911. doi:10.2903/j.efsa.2017.4911.

Eliášová, M., Pospiech, M., Tremlová, B., Kubíčková, K., Jandásek, J., 2012. Native and modified starches in meat products-detection of raw materials using microscopy methods. Maso Int. 2, 101–108.

Gallier, S., Gordon, K.C., Singh, H., 2012. Chemical and structural characterisation of almond oil bodies and bovine milk fat globules. Food Chem. 132 (4), 1996–2006. doi:10.1016/j.foodchem.2011.12.038.

Gierczynski, I., Guichard, E., Laboure, H., 2011. Aroma perception in dairy products: the roles of texture, aroma release and consumer physiology. A review. Flavour Fragr. J. 26 (3), 141–152. doi:10.1002/ffj.2036.

Grand View Research, 2020. Vegan yogurt market size, share & trends analysis report by product (Soy, Almond, Rice). In: By Distribution Channel (Hypermarket, Supermarket, Convenience Stores, Specialty Stores, Online). By Region, And Segment Forecasts, pp. 2020–2027.

Grasso, N., Alonso-Miravalles, L., O'Mahony, J.A., 2020. Composition, physicochemical and sensorial properties of commercial plant-based yogurts. Foods 9 (3), 252. doi:10.3390/foods9030252.

Greis, M., Sainio, T., Katina, K., Kinchla, A.J., Nolden, A., Partanen, R., Seppä, L., 2020. Dynamic texture perception in plant-based yogurt alternatives: identifying temporal drivers of liking by TDS. Food Qual. Prefer. 86, 104019. doi:10.1016/j.foodqual.2020.104019.

Jeske, S., Zannini, E., Arendt, E.K., 2018. Past, present and future: the strength of plant-based dairy substitutes based on gluten-free raw materials. Food Res. Int. 110, 42–51. doi:10.1016/j.foodres.2017.03.045.

Kumar, A., Stickland, A.D., Scales, P.J., 2012. Viscoelasticity of coagulated alumina suspensions. Korea-Aust. Rheol. J. 24 (2), 105–111. doi:10.1007/s13367-012-0012-3.

Lee, J., Townsend, J.A., Thompson, T., Garitty, T., De, A., Yu, Q., Peters, B.M., Wen, Z.T., 2018. Analysis of the cariogenic potential of various almond milk beverages using a Streptococcus mutans biofilm model in vitro. Caries Res. 52 (1–2), 51–57. doi:10.1159/000479936.

Lee, W.J., Lucey, J.A., 2010. Formation and physical properties of yogurt. Asian-Aust. J. Anim. Sci. 23 (9), 1127–1136. doi:10.5713/ajas.2010.r.05.

Li, Y., Shoemaker, C.F., Ma, J., Moon, K.J., Zhong, F., 2008. Structure-viscosity relationships for starches from different rice varieties during heating. Food Chem. 106 (3), 1105–1112. doi:10.1016/j.foodchem.2007.07.039.

Li, J.Y., Yeh, A.I., 2001. Relationships between thermal, rheological characteristics and swelling power for various starches. J. Food Eng. 50 (3), 141–148. doi:10.1016/S0260-8774(00)00236-3.

Matignon, A., Moulin, G., Barey, P., Desprairies, M., Mauduit, S., Sieffermann, J.M., Michon, C., 2014. Starch/carrageenan/milk proteins interactions studied using multiple staining and confocal laser scanning microscopy. Carbohydr. Polym. 99, 345–355. doi:10.1016/j.carbpol.2013.09.002.

Mennah-Govela, Y.A., Bornhorst, G.M., 2021. Food buffering capacity: quantification methods and its importance in digestion and health. Food Funct. 12 (2), 543–563. doi:10.1039/D0FO02415E.

Nguyen, H.T.H., Ong, L., Lefèvre, C., Kentish, S.E., Gras, S.L., 2014. The microstructure and physicochemical properties of probiotic buffalo yoghurt during fermentation and storage: a comparison with bovine yoghurt. Food Bioproc. Tech. 7 (4), 937–953. doi:10.1007/s11947-013-1082-z.

Nguyen, P., Kravchuk, O., Bhandari, B., Prakash, S., 2017. Effect of different hydrocolloids on texture, rheology, tribology and sensory perception of texture and mouthfeel of low-fat pot-set yoghurt. Food Hydrocoll. 72, 90–104. doi:10.1016/j.foodhyd.2017.05.035.

Nik, A.M., Tosh, S.M., Woodrow, L., Poysa, V., Corredig, M., 2009. Effect of soy protein subunit composition and processing conditions on stability and particle size distribution of soymilk. LWT-Food Sci. Technol. 42 (7), 1245–1252. doi:10.1016/j.lwt.2009.03.001.

Ong, L., Dagastine, R.R., Kentish, S.E., Gras, S.L., 2011. Microstructure of milk gel and cheese curd observed using cryo scanning electron microscopy and confocal microscopy. LWT- Food Sci. Technol. 44 (5), 1291–1302. doi:10.1016/j.lwt.2010.12.026.

Pang, Z., Luo, Y., Li, B., Zhang, M., Liu, X., 2020. Effect of different hydrocolloids on tribological and rheological behaviors of soymilk gels. Food Hydrocoll. 101, 105558. doi:10.1016/j.foodhyd.2019.105558.

Peighambardoust, S., Van der Goot, A., Van Vliet, T., Hamer, R., Boom, R., 2006. Microstructure formation and rheological behaviour of dough under simple shear flow. J. Cereal Sci. 43 (2), 183–197. doi:10.1016/j.jcs.2005.10.004.

Prakash, S., Tan, D.D.Y., Chen, J., 2013. Applications of tribology in studying food oral processing and texture perception. Food Res. Int. 54 (2), 1627–1635. doi:10.1016/j.foodres.2013.10.010.

Rao, M., Tattiyakul, J., 1999. Granule size and rheological behavior of heated tapioca starch dispersions. Carbohydr. Polym. 38 (2), 123–132. doi:10.1016/S0144-8617(98)00112-X.

Salaün, F., Mietton, B., Gaucheron, F., 2005. Buffering capacity of dairy products. Int. Dairy J. 15 (2), 95–109. doi:10.1016/j.idairyj.2004.06.007.

Sathe, S.K., Wolf, W.J., Roux, K.H., Teuber, S.S., Venkatachalam, M., Sze-Tao, K.W., 2002. Biochemical characterization of amandin, the major storage protein in almond (*Prunus dulcis L.*). J. Agric. Food Chem. 50 (15), 4333–4341. doi:10.1021/jf020007v.

Shen, Z., Liu, Z., Rui, X., Chen, X., Jiang, M., Dong, M., 2021. Effects of fat content on the textural and in vivo buccal breakdown properties of soy yogurt. J. Texture Stud. 52 (3), 334–346. doi:10.1111/jtxs.12584.

Shi, H., Kraft, J., Guo, M., 2020. Physicochemical and microstructural properties and probiotic survivability of symbiotic almond yogurt alternative using polymerized whey protein as a gelation agent. J. Food Sci. 85 (10), 3450–3458. doi:10.1111/1750-3841.15431.

Sim, S.Y., Hua, X.Y., Henry, C.J., 2020. A novel approach to structure plant-based yogurts using high pressure processing. Foods 9 (8), 1126. doi:10.3390/foods9081126.

Szparaga, A., Tabor, S., Kocira, S., Czerwińska, E., Kuboń, M., Płóciennik, B., Findura, P., 2019. Survivability of probiotic bacteria in model systems of non-fermented and fermented coconut and hemp milks. Sustainability 11 (21), 6093. doi:10.3390/su11216093.

Tamime, A.Y., Hickey, M., Muir, D.D., 2014. Strained fermented milks–A review of existing legislative provisions, survey of nutritional labelling of commercial products in selected markets and terminology of products in some selected countries. Int. J. Dairy Technol. 67 (3), 305–333. doi:10.1111/1471-0307.12147.

Tasneem, M., Siddique, F., Ahmad, A., Farooq, U., 2014. Stabilizers: indispensable substances in dairy products of high rheology. Crit. Rev. Food Sci. Nutr. 54 (7), 869–879. doi:10.1080/10408398.2011.614702.

Tipvarakarnkoon, T., Blochwitz, R., Senge, B., 2008. Rheological properties and phase change behaviors of coconut fats and oils. Ann. Trans. Nordic Rheol. Soci. 16, 159–166.

Tournier, C., Sulmont-Rossé, C., Guichard, E., 2007. Flavour Perception: Aroma, Taste and Texture Interactions.

Trontel, A., Baršić, V., Slavica, A., Santek, B., Novak, S., 2010. Modelling the effect of different substrates and temperature on the growth and lactic acid production by lactobacillus amylovorus DSM 20531 T in batch process. Food Technol. Biotechnol. 48 (3). https://urn.nsk.hr/urn:nbn:hr:159:642072.

Truong, T., Palmer, M., Bansal, N., Bhandari, B., 2016. Effect of Milk Fat Globule Size on the Physical Functionality of Dairy Products. Cham, Switzerland doi:10.1007/978-3-319-23877-7.

Tyl, C., Sadler, G.D., Nielsen, S.S., 2017. pH and Titratable acidity. In: Food Analysis. Springer International Publishing, pp. 389–406. doi:10.1007/978-3-319-45776-5_22.

Wolf, W.J., Sathe, S.K., 1998. Ultracentrifugal and polyacrylamide gel electrophoretic studies of extractability and stability of almond meal proteins. J. Sci. Food Agric. 78 (4), 511–521.

Wood, F., 1968. Psychophysical Studies on the Consistency of Liquid Foods. Rheology and Texture of Food Stuffs. SCI Monogr. 27, 40–49.

Yada, S., Huang, G., Lapsley, K., 2013. Natural variability in the nutrient composition of California-grown almonds. J. Food Compos. Anal. 30 (2), 80–85. doi:10.1016/j.jfca.2013.01.008.

Yada, S., Lapsley, K., Huang, G., 2011. A review of composition studies of cultivated almonds: macronutrients and micronutrients. J. Food Compos. Anal. 24 (4–5), 469–480. doi:10.1016/j.jfca.2011.01.007.

Yahaya, A., Taiwo, O., Shittu, T., Yahaya, L., Jayeola, C., 2012. Investment in cashew kernel oil production; cost and return analysis of three processing methods. Am. J. Econ. 2 (3), 45–49. doi:10.5923/j.economics.20120203.04.

Yazici, F., Alvarez, V., Hansen, P., 1997. Fermentation and properties of calcium-fortified soy milk yogurt. J. Food Sci. 62 (3), 457–461. doi:10.1111/j.1365-2621.1997.tb04406.x.

Yilmaz- Ersan, L., Topcuoglu, E., 2021. Evaluation of instrumental and sensory measurements using multivariate analysis in probiotic yogurt enriched with almond milk. J. Food Sci. Technol. 59, 133–143. doi:10.1007/s13197-021-04994-w.

Zhang, B., Selway, N., Shelat, K.J., Dhital, S., Stokes, J.R., Gidley, M.J., 2017. Tribology of swollen starch granule suspensions from maize and potato. Carbohydr. Polym. 155, 128–135. doi:10.1016/j.carbpol.2016.08.064.

Zhao, J., Bhandari, B., Gaiani, C., Prakash, S., 2021. Physicochemical and microstructural properties of fermentation-induced almond emulsion-filled gels with varying concentrations of protein, fat and sugar contents. Curr. Res. Food Sci. 4, 577–587. doi:10.1016/j.crfs.2021.08.007.

Zhao, J., Bhandari, B., Gaiani, C., Prakash, S., 2022. Altering almond protein function through partial enzymatic hydrolysis for creating gel structures in acidic environment. Curr. Res. Food Sci. 5, 653–664. doi:10.1016/j.crfs.2022.03.012.

Ziegler, G.R., Thompson, D.B., Casasnovas, J., 1993. Dynamic measurement of starch granule swelling during gelatinization. Cereal Chem. 70 (3), 247–251.